

## Original Article

# The antifibrotic effects of the novel compound gorse isoflavone alkaloid on chemical liver injury in rats

Yang-Wen Ai<sup>1,2</sup>, Fang-Cheng Fan<sup>1</sup>, Hua Liu<sup>1</sup>, Xiao-Jie Shi<sup>1</sup>, Ke-Qin Li<sup>1</sup>, Qing-Shan Liu<sup>1,2</sup>, Hui Jiang<sup>3</sup>

<sup>1</sup>School of Pharmacy, Minzu University of China, Beijing 100000, China; <sup>2</sup>Center on Translational Neuroscience, Minzu University of China, Beijing 100000, China; <sup>3</sup>Department of Otolaryngology and Stomatology, The Second Affiliated Hospital of Shandong First Medical University, Tai'an 271000, Shandong, China

Received April 9, 2022; Accepted July 5, 2022; Epub August 15, 2022; Published August 30, 2022

**Abstract:** Objective: Liver fibrosis is a frequently occurring liver injury which lacks of effective treatment clinically. Here, we investigated the protective effects of a novel compound Gorse isoflavone alkaloid (GIA) against liver fibrosis. Methods: Totally forty rats were randomly divided into four groups. Then we established a model of liver fibrosis induced by the intragastric administration of carbon tetrachloride (CCl<sub>4</sub>). This treated group was followed by the intragastric administration of GIA and colchicine. Then the liver index and spleen index, and liver function indexes were detected by kit. Western blotting assay was performed to estimate the expression of Transforming Growth Factor-β1 (TGF-β1) and related proteins. Tissue fibrosis was observed by Masson staining. Results: Our results suggested that GIA reduced the deposition of collagen fibres and the fibrosis index hydroxyproline (Hyp) of liver tissue. Furthermore, we found that GIA significantly decreased the expression of Transforming Growth Factor-β1 (TGF-β1) and the ratio of p-smad2/3 to smad2/3, enhanced the level of superoxide dismutase (SOD), and decreased the concentration of malonic dialdehyde (MDA) in the liver. Conclusions: Our findings revealed that GIA has a beneficial effect to resist the liver fibrosis, and could be ideal for potential use in antifibrotic drugs for the liver.

**Keywords:** Liver fibrosis, extracellular matrix, TGF-β1, TGF-β1/Smad2/3, HSC

## Introduction

*Sophora alopecuroides* L. (*Sophora alopecuroides*), also known as herb locust or bitter bean root, is a perennial herb in the Fabaceae and *Sophora* genera. *Sophora alopecuroides* L. is about 1 m tall, with branches covered with white or greyish white pilose or appressed pilose. *Alopecia alopecia* grows at the edge of arid desert and grassland at the altitude of 500-1600 m, and has strong resistance to cold, drought, saline-alkali, and sand. as well as other special properties. The roots, stems, seeds and even the whole plant of *Sophora alopecuroides* can be used as medicine, with anti-inflammatory, anti-allergy, anti-virus, anti-tumor effects etc. [1, 2].

Dietary therapy has been popular in recent years, and there has been increasing interest in utilization of natural products and functional foods for the treatment of damaged livers [3, 4]. *Sophora alopecuroides* L. and *angelica*

*decursiva* (Miq.) f. *decursiva* are very popular foods in eastern countries. They show a wide range of bioactivity. As a traditional liver-protecting food, *angelica* is common in restaurants and canteens and is consumed daily as a functional food by more than 100 million people in China, Japan, and South Korea. However, the mechanism remains unclear.

Fibrosis of the liver due to chronic liver injury can be caused by a variety of factors. Several conditions affecting the liver can be caused by excessive alcohol consumption, such as non-alcoholic steatohepatitis, viral hepatitis, autoimmune hepatitis, non-alcoholic fatty liver disease, and cholestatic liver disease [5]. The formation of fibrous scars in the liver results from the fibrotic response of the liver and the accumulation of extracellular matrix (ECM) components [6, 7].

The early stage of liver cirrhosis is liver fibrosis. Liver cirrhosis is currently irreversible; however,

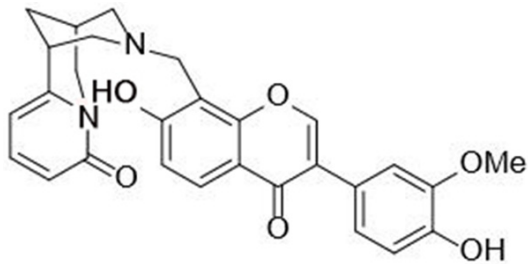


**Figure 1.** Structure of the gorse isoflavone alkaloid.

liver fibrosis can be reversed with appropriate treatment [8]. Hence, effectively reversing the occurrence and development of liver fibrosis has great significance for preventing end-stage liver disease [9]. However, the current treatment strategy for liver fibrosis has many limitations and is unable to completely inhibit the inflammatory response and degrade the hyperproliferative fibrous tissue [10]. Although colchicine has been reported to have antifibrotic effects on liver, its clinical application is limited by factors such as price, curative effect, and side effects. Therefore, new treatments for liver fibrosis are needed urgently.

In this study, we studied these foods using targeted screening and isolated the novel compound Gorse isoflavone alkaloid (GIA) (**Figure 1**) as the active ingredient. We hypothesized that GIA prevents liver fibrosis through inhibiting activation of hydroxyproline (Hyp) and expression of Transforming Growth Factor- $\beta$ 1 (TGF- $\beta$ 1), which serves as an antioxidant. Since there is currently no fully effective drug for the treatment and/or prevention of liver fibrosis, this new compound, modified from edible medicinal plants, may have strong potential to be used in future as antifibrotic strategy as well as functional foods to treat liver fibrosis.

## Materials and methods

### Animals

Adult male specific-pathogen-free (SPF) Wistar rats, weighing  $200 \text{ g} \pm 20 \text{ g}$  were purchased from the Breeding Ground of Laboratory Animal Research Institute, Chinese Academy of Medical Sciences (animal lot number: SCXK, Beijing 2005-0013). The rats were kept in a regular environment at  $15\text{-}25^\circ\text{C}$  and 55% relative humidity under a 12 h dark/light cycle. The

rats had an acclimatization period of at least one week preceded their use.

All animal experiments complied with the National Institutes of Health guide for the care and use of Laboratory animals (NIH Publications No. 8023), and approved by Biological and Medical Ethics Committee, Minzu University of China (ECMUC2019001 A0).

### Materials

Gorse isoflavone alkaloid was synthesized by the laboratory group of the present study. Colchicine was purchased from Fluka Products, America. Analytical grade carbon tetrachloride (Lot No. 20080525), haematoxylin, acid fuchsin, ponceau red and formaldehyde solution were all purchased from Sinopharm Group Chemical Reagent Co. Ltd, China. We obtained alanine aminotransferase (ALT), aspartate aminotransferase (AST) and albumin (ALB) kits (Lot No. 070151), a globulin (GLB) Kit (Lot No. 070141), malonic dialdehyde (MDA) Kit (Lot No. A001-7-1), superoxide dismutase (SOD) Kit (Lot No. A001-3-2) and a Hyp kit (Lot No. 20080505) from Sino Biotech Co., Ltd. Nanjing Jiancheng Bioengineering Research Institute, China. TGF- $\beta$ 1 rabbit anti-mouse polyclonal antibody (Lot No. 20080600) was purchased from Wuhan Boshide Bioengineering Co., Ltd, and a DAB color reagent kit from Wuhan Boshide Company, China. Trizol reagent (Lot No. 15596026, Life Technologies), cDNA Synthesis kit (AE311-03, TransGen Biotech, Beijing, China). GAPDH (ab181602, Abcam), Smad2/3 and phosphorylated Smad2/3 Polyclonal Antibody (Affinity, AF3367).

### Experimental treatment

The rats were randomly divided into four groups, with ten rats per group. The rats in the control group were fed 2 ml/kg of peanut oil two times a week, and 90 mg kg/d of distilled water once a day, for six weeks. The rats in the liver fibrosis model group were fed with a 1:1 mixture of carbon tetrachloride ( $\text{CCl}_4$ ) and 2 ml/kg of peanut oil by gavage twice a week and 90 mg kg/d of distilled water by gavage once a day for six weeks. The rats in the GIA group were fed 2 ml/kg of an equal mixture of  $\text{CCl}_4$  and peanut oil by gavage two times a week, and 90 mg kg/d of GIA for six weeks. The rats in the colchi-

cine group were fed 2 ml/kg of an equal mixture of  $\text{CCl}_4$  and peanut oil by gavage two times a week and 0.2 mg/kg/d of colchicine for six weeks.

#### *Sample collection*

The rats were put on a fast for 24 hours prior to being sacrificed. They were then weighed, anaesthetized with 3% pentobarbital sodium (1.5 ml/kg) and 4 ml of blood was taken from the abdominal aorta. The blood was centrifuged at 3500 r/min for 10 min, and serum was taken to be tested. The animal was then sacrificed, and the liver specimen was quickly cut, placed in iced saline and washed thoroughly. The liver and spleen were both weighed. 1 cm×1 cm×0.2 cm samples of remaining liver tissues were collected and fixed in a 10% solution of neutral formaldehyde for examination.

#### *Determination of liver index and spleen index*

The Wistar rats were weighed and then sacrificed. The liver and spleen were stripped and weighed separately. The results were expressed as liver index (liver weight/weight) and spleen index (spleen weight/weight).

#### *Determination of liver function indexes*

The detection of ALT, AST, ALB and GLB after the sample is added according to the kit instructions, the automatic biochemical analyzer automatically detects and calculates the results.

#### *Observation of liver pathology*

We embedded the paraffin-fixed liver tissues, sectioned them, and stained them with Masson. The pathological changes were then observed under a light microscope and photographed. We took the circumference and the central area of each slice and selected the areas with the most collagen fibre content. Each image contained a manifold area. A computer image analysis system was used to capture the images with photomicrography and these were entered into the image analysis system for grey-scale transformation to separate the coloured collagen fibre areas from the background. Automatic recordings were taken of both the coloured area and the total area. The percentage of the total area made up of collagen fibre was measured under a 100×

microscope. The calculation method was: collagen fibre area/liver tissue area ×100%. Average values were taken.

#### *Determination of hydroxyproline in liver tissue by alkaline hydrolysis*

80-100 mg of liver tissue was weighed out into a test tube and 1 ml of hydrolysate was added. These were mixed well. After capping, the water bath was hydrolysed for 20 minutes, adjusting the pH to around 6.0-6.8. When each test tube had been cooled with water, one drop of indicator was added to each tube, which was then shaken well. We then added 1.0 ml of pH control solution to each tube and mixed well (the solution was red at this time). We aspirated the pH-adjusted B liquid with a 200- $\mu$ l sampler and carefully added the pH-adjusted B liquid dropwise to each tube. After each drop of the liquid, we mixed well until the colour of the indicator in the liquid turned yellow-green. At this time, the pH was around 6.0-6.0. We then added distilled water to bring the liquid to 10 ml and mixed well again. We took 3-4 ml of diluted hydrolysate and mixed it with the appropriate activated carbon at 3500 rpm for 10 minutes. We then carefully took 1 ml of supernatant for testing.

#### *Immunohistochemistry*

In 10 mmol/L citrate buffer (pH 6.0), tissue sections were microwaved for 15 minutes to unmask antigens. Immunostaining was performed using avidin biotinylated enzyme complexes and antibodies. The controls were polyclonal nonimmune IgG (immunoglobulin G) of equivalent concentrations. Following incubation with the appropriate biotin-conjugated secondary antibody and streptavidin solution, we used 3, 3'-diaminobenzidine tetrahydrochloride as the chromogen to develop the colours. Counterstained sections were carried out with Gill-2 haematoxylin. Increasing concentrations of ethanol and xylene were used to dehydrate the sections after staining (which is transparent and was sealed with neutral gum). The sections were then observed under a microscope.

#### *The extraction of RNA and quantitative RT-PCR*

50 mg of liver tissue was taken from each sample, total RNA of liver tissue was extracted with TRI-Reagent reagent, and residual genom-

**Table 1.** Comparison of weight increase of rats in each group ( $X \pm SD$ )

Group	n	Weight changes (g)
Control	10	164±33
Model	10	99±45**
Gorse isoflavone alkaloid	10	147±27 <sup>#</sup>
Colchicine	10	107±40 <sup>#</sup>

Weight changes. Compared with the control group  
 \*\* $P < 0.01$ , compared with the model group <sup>#</sup> $P < 0.05$ ,  
 n=10.

ic DNA was digested with RNase-free water. We measured the absorbance at OD260/OD280 of the sample to determine its RNA content. The 40  $\mu$ l reverse transcription reaction system contains 0.5  $\mu$ g of oligo (dT)15 primer, 1 mM of dNTP, 15U of AMV reverse transcriptase, 1U/ $\mu$ l of RNase inhibitor, 5 mM of MgCl<sub>2</sub>, 10 mM of Tris-HCl (pH 8.0), 50 mM of KCl, and 0.1% Triton X-100. In addition, the reverse transcription reaction system was denatured at 70°C for 10 minutes, incubated at 42°C for 60 minutes, and then heated at 95°C for 5 minutes to stop the reaction. PCR was conducted using primers listed in [Table S1](#) to amplify fragments specific to TGF- $\beta$ 1, Smad2, Smad3, and GAPDH from first strand cDNA. By analyzing the sequences of the PCR products, the identity of the resulting products was confirmed. In the same tissue samples, the expression levels of all transcripts were normalized to GAPDH mRNA levels.

#### Western blotting assay

After the protein concentration was determined, the protein volume was calculated according to the protein loading volume and the protein concentration of the cell sample, and the protein loading buffer of 5 times the relative volume was added, and the protein cracking solution was used to replenish the remaining volume, so that the protein loading buffer was diluted to 1 time. After denaturation, thirty  $\mu$ g protein was isolated by 10% sodium dodecyl sulfate polyacrylamide gel electrophoresis (SDS-PAGE), wet transferred to nitrocellulose (NC) membrane, and sealed with 5% skimmed milk powder Tris-HCl buffer salt solution (TBST) at room temperature for 2 h. Primary antibodies of TGF- $\beta$ 1 (44 kD), Smad2/3 (48 kD), p-Smad2/3 (48 kD) and GAPDH (36 kD) were incubated at 4°C overnight. After reacting with ECL chemiluminescence solution, the imaging system carried out automatic exposure, and the gray value of each color band was mea-

sured by Image J software for analysis. The ratio of the target protein to internal reference gray value in each group was used as the relative quantity of protein expression in each group.

#### Analyses statistical

$P < 0.05$  was considered statistically significant. All statistical analyses were performed using SPSS 20.0 software, along with one-way ANOVA. Data are presented as mean  $\pm$  standard deviation (SD).

## Results

### Observation and weight changes

The control group was generally in good condition, with shiny, white hair, normal appetite and an average weight gain of 164 g over the six weeks. The activity of the model group gradually decreased over the administration time, and the hair became messy, dark and yellow. The animals' behaviour indicated depression. Food intake was reduced, urine colour was yellow, and there was diarrhoea. However, rats of the GIA group and the colchicine group were generally in good condition, normal appetite. The body weight of the GIA group increased by an average of 147 g, which was significantly different from the model group and the colchicine group (**Table 1**).

### Effects of GIA on liver function indexes

In comparison with the control group, the concentration of serum ALT and AST in the tissue of the model group was obviously increased. In comparison with the model group, GIA showed a significant reduction in the release of ALT and AST. This reduction was significantly greater in the GIA group than in the colchicine group (**Figure 2A**). Compared with the control group, the serum ALB content of the model group was significantly reduced, and the ratio of albumin to GLB was reduced. The GIA group showed higher levels of serum ALB and a greater proportion of the model group of GLB than the model group (**Figure 2B, 2C**).

The liver index and spleen index of the model group were significantly decreased to those of the control group. Compared with the indexes of the model group and the colchicine group, those of the GIA group decreased significantly (**Figure 2D**).

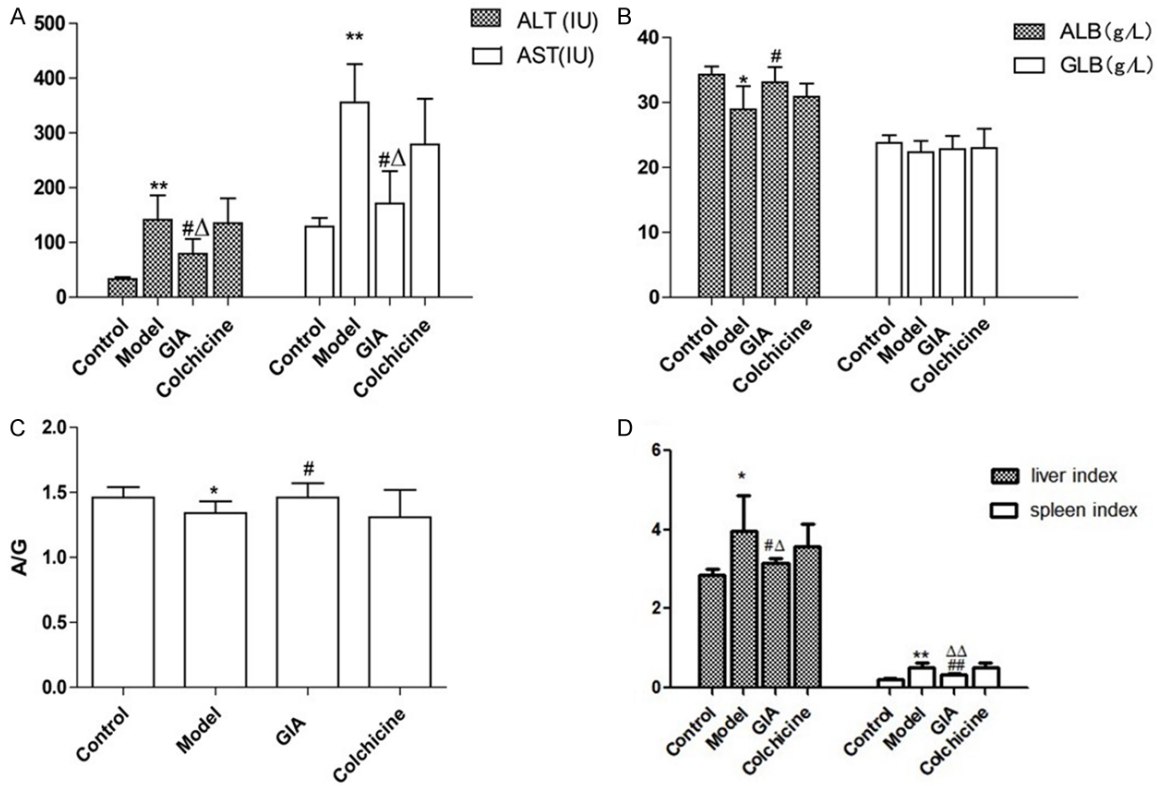


**Figure 2.** A. Changes in serum alanine aminotransferase (ALT) and aspartate aminotransferase (AST). B. Changes in serum albumin (ALB) and globulin (GLB) levels. C. Comparison of ALB and GLB levels. D. Liver index and spleen index. Compared with the control group \* $P < 0.05$ , \*\* $P < 0.01$ , compared with the model group # $P < 0.05$ , ## $P < 0.01$ , compared with the colchicine group Δ $P < 0.05$ , ΔΔ $P < 0.01$ ,  $n = 10$  (GIA, Gorse isoflavone alkaloid).

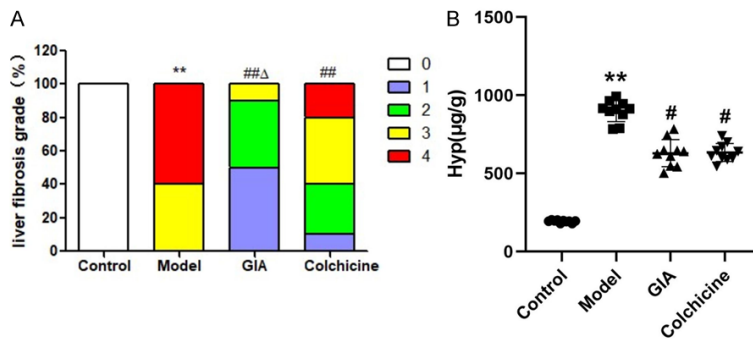


**Figure 3.** A. Liver fibrosis grades. B. Concentrations of hydroxyproline (Hyp) in the liver tissue. Compared with the control group \*\* $P < 0.01$ , compared with the model group # $P < 0.05$ , ## $P < 0.01$ , compared with the colchicine group Δ $P < 0.05$ ,  $n = 10$  (GIA, Gorse isoflavone alkaloid).

The results are shown in **Figure 3A**. The grades of liver fibrosis found in the tissue samples of the four groups are shown in **Figure 3B**. The liver fibrosis grade of the model group was significantly higher than that of the control group ( $P < 0.01$ ). The liver fibrosis classification of the GIA group was significantly different from that of the model group and the colchicine group. GIA treated rats had a significantly reduced liver fibrosis grade.

#### The effects of GIA on the Hyp and grading of rat liver fibrosis

The concentration of Hyp in the liver tissue of the model group was much higher than that of the control group ( $P < 0.01$ ) and the value of Hyp in the GIA group and colchicine groups was significantly lower than that of the model group.

Liver fibrosis is divided into five stages, the first stage (0) means no liver fibrosis; The second stage (1) refers to the fibrosis around the sink area and the sink area, as well as the fibrosis around the hepatic sinuses or the fibrous scar in the lobule; The third stage (2) refers to the formation of fibrous septa within the lobule, and multiple fibrous septa can be seen; The

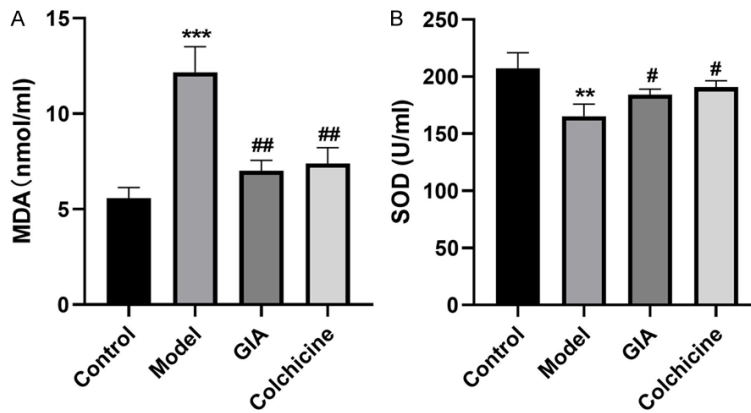


**Figure 4.** GIA alleviated oxidative stress injury in liver fibrosis model rats. A. Concentrations of, and malonic dialdehyde (MDA) in liver tissue. B. The level of superoxide dismutase (SOD) in liver tissue. Compared with the control group  $**P<0.01$ ,  $***P<0.001$ , compared with the model group  $\#P<0.05$ ,  $##P<0.01$ ,  $n=3$  (GIA, Gorse isoflavone alkaloid).

fourth stage (3) refers to the formation of a large number of fibrous septa, and destruction of liver lobules, resulting in lobule structural disorder; The fifth stage (4) refers to early cirrhosis, with the formation of pseudo lobules, inter septal collagen and elastic fibers remodeled in parallel.

#### *GIA alleviated oxidative stress injury in liver fibrosis model rats*

Oxidative stress is an important cause of the death of hepatocyte in liver fibrosis. GIA could act as an antioxidant agent, as stated in the introduction. Hepatic tissue MDA and SOD levels were measured to evaluate the degree of oxidative stress damage and antioxidant capacity. The results (Figure 4A) showed that compared with the control group, the MDA level in Model group was significantly increased, and the change was significantly alleviated by GIA and the colchicine treatment ( $P<0.01$ ). Similarly, the concentration of SOD significantly reduced in the Model group, while GIA and the colchicine treatment significantly increased it (Figure 4B).

#### *Masson collagen staining*

Masson collagen staining colours collagen fibres blue, enabling examination of collagen fibre distribution under the microscope.

In the control group, only a small number of blue fibres were seen. These were around the thin, short blood vessels in the manifold area, as shown in Figure 5A. In the model group, col-

lagen fibres in the liver tissue extended outward along the manifold inflammatory necrosis areas to form fibrous spaces of varied thickness, dividing and surrounding the liver lobule, and creating further partially formed lobule, as shown in Figure 5B. In the GIA group, collagen fibres in liver tissue proliferated along with the inflammatory and necrotic areas, forming intermittent, thin fibrous spaces. There was no apparent pseudolobule formation, as shown in Figure 5C. Levels of collagen fibre formation in the colchicine group were greater than that in the GIA group but less than the model group and, as shown in Figure 5D.

Quantitative analysis indicated that collagen fibre formation in the liver tissue of rats in the model group was significantly greater than in the control group. The amount of collagen fibre in the liver tissue of the GIA group was significantly lower than that in the model group and colchicine group. The colchicine group also showed significantly less fibre formation than the model group (Figure 5E).

#### *The effect of GIA on the Hyp and TGF-β1 in liver fibrosis rats*

The positive substance for TGF-β1 expression was brown granules. There were no TGF-β1 positively stained cells in the liver tissue of the control group. In the model group, positively stained cells were seen in the confluent area and the fibrous septa, most of which were fusiform or irregular in shape. Macrophages, fibroblasts, and hepatic stellate cells were dominant, with an average of 17 positive stains per 200× field of view (Figure 6), which was significantly greater than for the control group. There were fewer cells stained with TGF-β1 in the GIA group and colchicine group compared with the model group.

#### *Effects of GIA on the expression of mRNA in liver.*

RT-PCR was performed using total RNA isolated from the livers of the rats in each group as a template for PCR amplification. As shown in

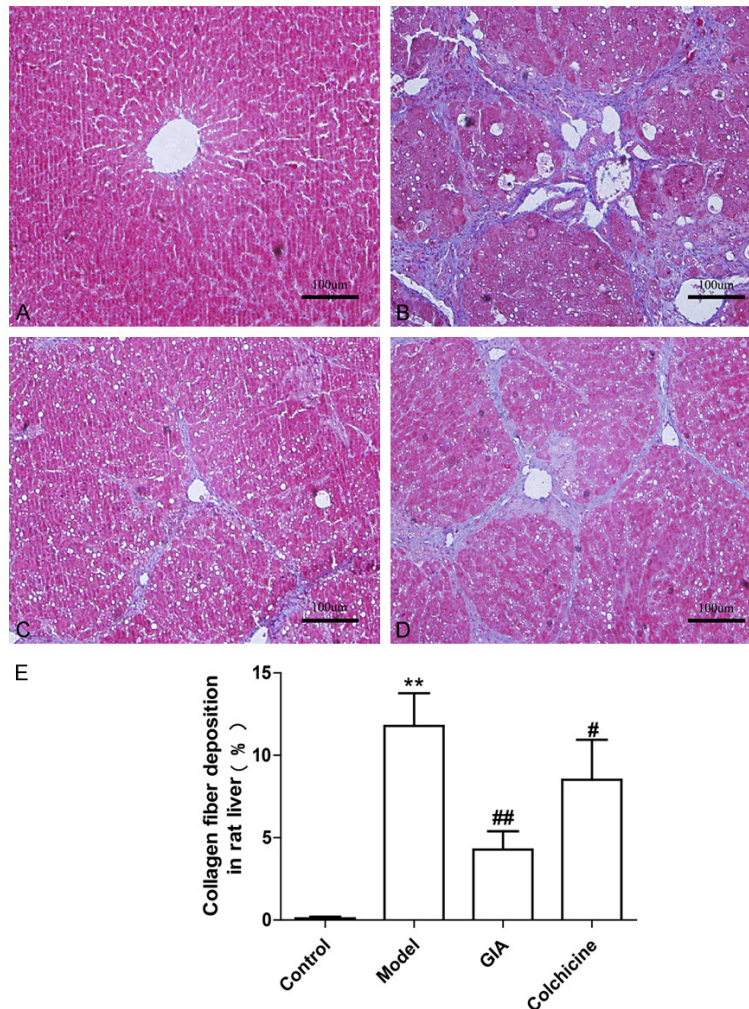


**Figure 5.** (A-D) Masson collagen staining (200 $\times$ ). (E) Quantitative analysis of collagen fibre deposition in the liver tissue of rats. Compared with the control group (A)  $**P<0.01$ , compared with the model group (B)  $\#P<0.05$ ,  $##P<0.01$ , compared with the colchicine group (D)  $\Delta P<0.05$ ,  $n=3$  (GIA, Gorse isoflavone alkaloid).

Figure S1, the expressions of TGF- $\beta$ 1, Smad2 and Smad3 mRNA in model group rats was significantly higher than those in the control group, and these mRNA levels were decreased in the rats treated with GIA. Meanwhile, the expression of TGF- $\beta$ 1, Smad2 and Smad3 mRNA was decreased in the Colchicine group as compared with the model group.

*TGF- $\beta$ 1 and p-Smad2/3 expression were down-regulated by GIA*

The expressions of TGF- $\beta$ 1 and p-smad2/3 in the liver of rats were detected. The results showed that the expressions of TGF- $\beta$ 1 and p-smad2/3 in the model group were significantly up-regulated when compared with the control

group (**Figure 7A, 7B**). The expressions of TGF- $\beta$ 1 and p-smad2/3 in the GIA group were down-regulated compared with the model group (**Figure 7B**). Although the expressions of smad2/3 among these groups showed no difference (**Figure 7C**), the ratio of p-smad2/3 to smad2/3 in the model group was apparently different from that of the GIA group and the Colchicine group (**Figure 7D**).

## Discussion

In this study, we investigated the antifibrotic effects and molecular mechanisms of the novel compound, gorse isoflavone alkaloid. Our data indicated that GIA is able to reduce the deposition of collagen fibres and the fibrosis index Hyp of liver tissue, with resultant antifibrotic effects on the liver.

Chemical liver injury is caused by alcohol, toxic substances in the environment and drugs. It is a precursor to various liver diseases, including liver fibrosis, cirrhosis, liver cell necrosis, and liver cancer. Since the aetiology of liver damage includes factors such as excessive drinking and drug abuse,

some people are more likely to be exposed to hepatotoxic substances to a degree that exceeds the metabolic capacity of the body, resulting in liver damage and, potentially, cause alcohol-induced liver damage, such as hepatic fibrosis and liver cancer [11].

Liver fibrosis is the pathological process of abnormal deposition of collagen and other fibrous tissue in the liver. During fibrosis, hepatocytes (HC) undergo necrosis and inflammatory stimulation and this causes the deposition and degradation of the ECM of collagen and other cells [12].

TGF- $\beta$ 1 is the core substance that regulates the occurrence and development of liver fibrosis

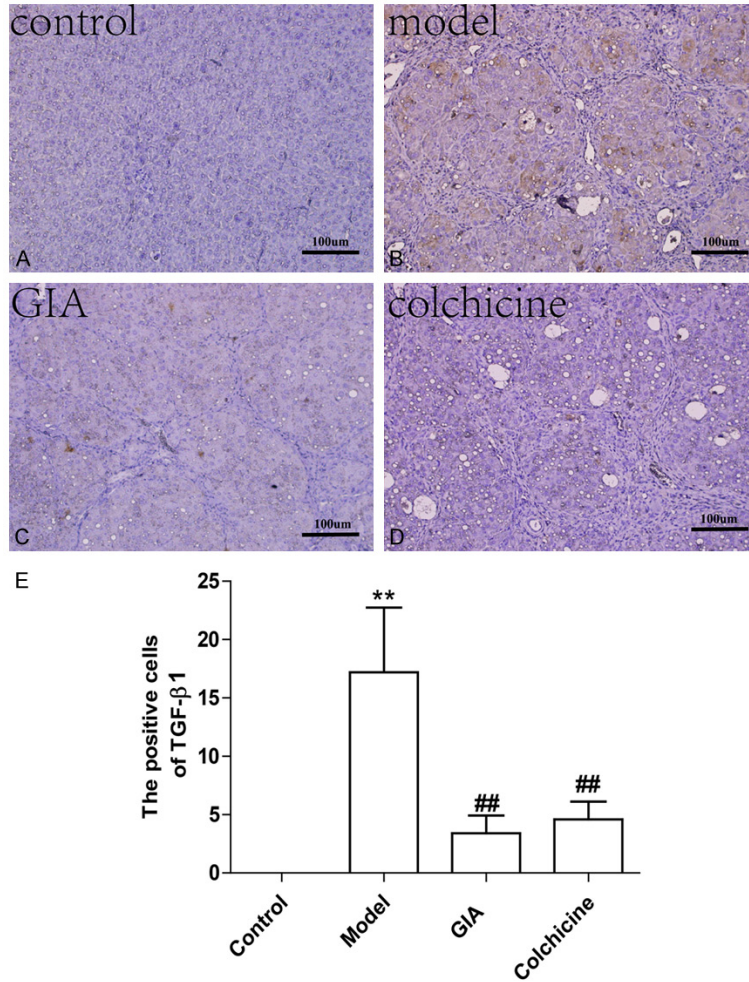


**Figure 6.** (A-D) Positive Transforming Growth Factor-β1 (TGF-β1) cells. (E) Quantitative analysis the positive TGF-β1 cells by immunohistochemical. Compared with the control group (A) \*\* $P < 0.01$ , compared with the model group (B) ## $P < 0.01$ ,  $n = 10$  (GIA, Gorse isoflavone alkaloid).

[13, 14]. TGF-β1 is a group of polypeptides with multiple biological functions, including a crucial role in regulation of cell proliferation and differentiation [15-17]. It is involved in the process of the cell cycle, the formation of blood vessels and embryos, the induction of apoptosis and immune regulation [18-20]. A lot of cells in the liver can produce TGF-β1 [21]. These include hepatic stellate cells (HSC), Kupffer cells, endothelial cells, blood-derived T lymphocytes and platelets.

TGF-β1 plays a significant role in liver fibrosis by converting HSCs to myfibroblasts (MFBs). At the same time, new HSC continues to secrete TGF-β1, which activates more HSC, creating a vicious circle and accelerating the progress of the fibrosis [22, 23]. TGF suppresses hepatocyte regeneration by inhibiting hepatocyte DNA

synthesis. It also induces hepatocyte apoptosis and the injured hepatocytes release large amounts of proline oxidase required for collagen synthesis and secretes TGF-β1 [24]. The TGF-β1 stimulates the synthesis of liver collagen and fibronectin at the level of transcription and translation while inhibiting the synthesis and secretion of various hydrolases. This increases the expression of tissue inhibitors of metalloproteinase (TIMP) and other protease inhibitors, antagonising the degradation of ECM, and promoting continuous deposition of ECM in the liver [25-27].

The TGF-β1/smad2/3 signaling pathway has a strong association with fibrosis and angiogenesis. Smad signal transduction pathway mediates collagen synthesis induced by TGF-β1, which plays a key role in the development of liver fibrosis and recovery [24]. TGF-β1 exerts its biological and pathological activity through the TGF-β/Smad2/3 signaling pathway when activated [28]. To clarify the relationship of TGF-β/Smad2/3 signaling pathway with GIA for

liver fibrosis, the mechanisms by which GIA resisted CCl<sub>4</sub> induced fibrosis were investigated. The phosphorylation of Smad2/3 is the key to activate the TGF-β/Smad2/3 signaling pathway. Our findings suggested that TGF-β1 was downregulated after GIA treatment, and GIA further inhibited phosphorylated Smad2 and Smad3, decreasing the ratio of p-smad2/3 to smad2/3 but no difference of smad2/3 among groups. According to our findings, GIA inhibits TGF-β/Smad2/3 signaling, which is consistent with previous findings that GIA to be antifibrotic in hepatic fibrosis.

Hyp is a unique amino acid of collagen. The level of Hyp is indicative of the amount of collagen in the liver and this indicates the degree of liver fibrosis. Measuring the level of Hyp in liver tissue is a common method for inferring

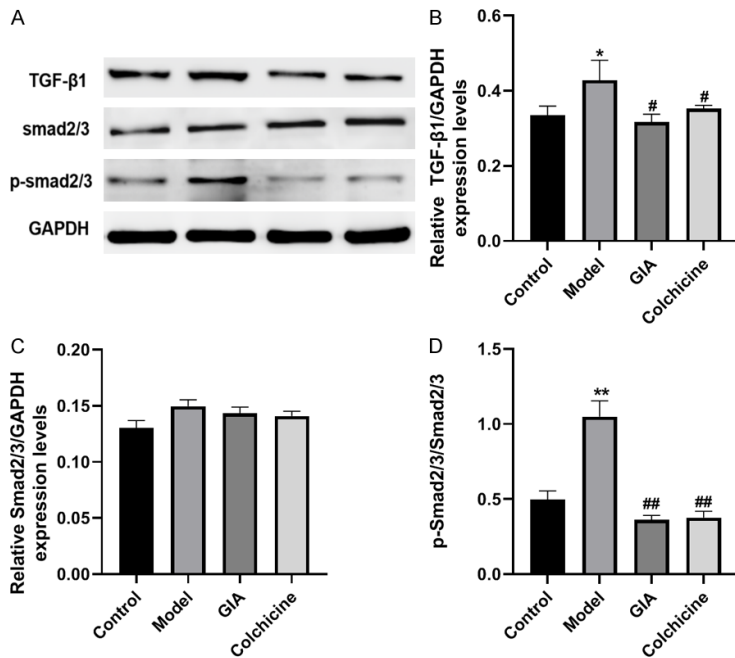


**Figure 7.** The expressions of Transforming Growth Factor-β1 (TGF-β1), smad2/3 and p-smad2/3 in the liver. (A-C) The expressions of TGF-β1, p-smad2/3 and smad2/3 were detected by western blot, GAPDH was used as an internal control. (D) The ratio of p-smad2/3 to smad2/3 was calculated based on the protein expressions of p-smad2/3 and smad2/3. Compared with the control group \* $P < 0.05$ , \*\* $P < 0.01$ , compared with the model group ## $P < 0.05$ , ### $P < 0.01$ ,  $n = 3$  (GIA, Gorse isoflavone alkaloid).

the collagen fibre levels [29]. In this study, rats with  $\text{CCl}_4$  induced liver fibrosis had significantly higher levels of Hyp than the healthy control group, indicating that collagen hyperplasia is very active. Rats with  $\text{CCl}_4$  induced liver fibrosis treated with GIA showed significantly lower Hyp levels. These results revealed that GIA can apparently reduce the degree of liver fibrosis in rats, which indicates that GIA may be helpful in resisting or reversing the progression of liver fibrosis.

As shown in **Figure 8**, our research showed that the mechanism by which GIA protects the liver might be due to the reduction of cytokine TGF-β1 expression in liver tissue. This would inhibit the HSC reaction and stellate cell activation, reducing the synthesis of collagen and other ECM and promoting their degradation. Those data implied that TGFβ/Smad2/3 pathways might be involved in mediating the anti-fibrosis activity of GIA in the liver. However, whether TGFβ/Smad2/3 pathways participate in mediating the anti-fibrosis effect of liver remain to be elucidated.

### Conclusion

In summary, gorse isoflavone alkaloid has a beneficial role in preventing liver fibrosis. It has a comprehensive pharmacological effect, various pathological targets and is an ideal antifibrotic novel compound. These findings indicate that gorse isoflavone alkaloid has considerable prospects in medicine and functional foods for future antifibrotic liver treatment.

### Acknowledgements

This work was supported by the Natural Science Foundation of

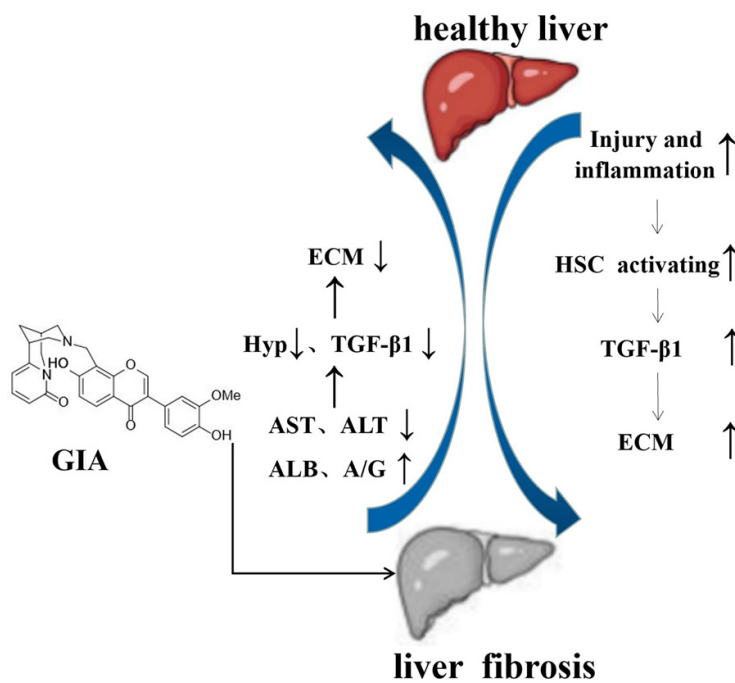


**Figure 8.** The mechanism by which GIA reduces liver fibrosis in rats (GIA, Gorse isoflavone alkaloid; ECM, Extracellular matrix; Hyp, Hydroxyproline; TGF-β1, Transforming Growth Factor-β1; ALT, Alanine aminotransferase; AST, Aspartate aminotransferase; ALB, Albumin; HSC, Hepatic stellate cells; A/G, ALB/GLB).

China (82174085) and Science and Technology Project of Tai'an, No. 2017NS0198.

#### Disclosure of conflict of interest

None.

**Address correspondence to:** Hui Jiang, Department of Otolaryngology and Stomatology, The Second Affiliated Hospital of Shandong First Medical University, Tai'an 271000, Shandong, China. E-mail: fyjianghui1@126.com

#### References

- [1] Liu Y, Xu Y, Ji W, Li X, Sun B, Gao Q and Su C. Anti-tumor activities of matrine and oxymatrine: literature review. *Tumour Biol* 2014; 35: 5111-5119.
- [2] Craig Plett D and Møller IS. Na(+) transport in glycophytic plants: what we know and would like to know. *Plant Cell Environ* 2010; 33: 612-626.
- [3] Gao L, Shan W, Zeng W, Hu Y, Wang G, Tian X, Zhang N, Shi X, Zhao Y, Ding C, Zhang F, Liu K and Yao J. Carnosic acid alleviates chronic alcoholic liver injury by regulating the SIRT1/ChREBP and SIRT1/p66shc pathways in rats. *Mol Nutr Food Res* 2016; 60: 1902-1911.
- [4] Wang F, Tipoe GL, Yang C, Nanji AA, Hao X, So KF and Xiao J. Lycium barbarum polysaccharide supplementation improves alcoholic liver injury in female mice by inhibiting stearyl-CoA desaturase 1. *Mol Nutr Food Res* 2018; 62: e1800144.
- [5] Aydın MM and Akçali KC. Liver fibrosis. *Turk J Gastroenterol* 2018; 29: 14-21.
- [6] Sun M and Kisseleva T. Reversibility of liver fibrosis. *Clin Res Hepatol Gastroenterol* 2015; 39 Suppl 1: S60-63.
- [7] Bataller R and Brenner DA. Liver fibrosis. *J Clin Invest* 2005; 115: 209-218.
- [8] Weng HL, Cai WM and Liu RH. Animal experiment and clinical study of effect of gamma-interferon on hepatic fibrosis. *World J Gastroenterol* 2001; 7: 42-48.
- [9] Yuan X, Wang B, Yang L and Zhang Y. The role of ROS-induced autophagy in hepatocellular carcinoma. *Clin Res Hepatol Gastroenterol* 2018; 42: 306-312.
- [10] Liaw YF. Reversal of cirrhosis: an achievable goal of hepatitis B antiviral therapy. *J Hepatol* 2013; 59: 880-881.
- [11] Gao B and Bataller R. Alcoholic liver disease: pathogenesis and new therapeutic targets. *Gastroenterology* 2011; 141: 1572-1585.
- [12] Han KH and Yoon KT. New diagnostic method for liver fibrosis and cirrhosis. *Intervirolgy* 2008; 51 Suppl 1: 11-16.
- [13] Ueberham E, Löw R, Ueberham U, Schönig K, Bujard H and Gebhardt R. Conditional tetracycline-regulated expression of TGF-beta1 in liver of transgenic mice leads to reversible intermediary fibrosis. *Hepatology* 2003; 37: 1067-1078.
- [14] Schnur J, Oláh J, Szepesi A, Nagy P and Thorgerirsson SS. Thioacetamide-induced hepatic fibrosis in transforming growth factor beta-1 transgenic mice. *Eur J Gastroenterol Hepatol* 2004; 16: 127-133.
- [15] Roberts AB, Piek E, Böttinger EP, Ashcroft G, Mitchell JB and Flanders KC. Is Smad3 a major player in signal transduction pathways leading to fibrogenesis? *Chest* 2001; 120: 43S-47S.
- [16] Akiyoshi S, Ishii M, Nemoto N, Kawabata M, Aburatani H and Miyazono K. Targets of transcriptional regulation by transforming growth factor-beta: expression profile analysis using oligonucleotide arrays. *Jpn J Cancer Res* 2001; 92: 257-268.
- [17] Blobel GC, Schiemann WP and Lodish HF. Role of transforming growth factor beta in human disease. *N Engl J Med* 2000; 342: 1350-1358.
- [18] Massagué J and Wotton D. Transcriptional control by the TGF-beta/Smad signaling system. *EMBO J* 2000; 19: 1745-1754.
- [19] Whitman M. Smads and early developmental signaling by the TGFbeta superfamily. *Genes Dev* 1998; 12: 2445-2462.
- [20] de Oliveira RC and Wilson SE. Fibrocytes, wound healing, and corneal fibrosis. *Invest Ophthalmol Vis Sci* 2020; 61: 28.
- [21] Derynk RJ, Jarrett JA, Chen EY, Eaton DH, Bell JR, Assoian RK, Roberts AB, Sporn MB and Goeddel DV. Human transforming growth factor-beta complementary DNA sequence and expression in normal and transformed cells. *Nature* 1985; 316: 701-705.
- [22] Schuster N and Kriegelstein K. Mechanisms of TGF-beta-mediated apoptosis. *Cell Tissue Res* 2002; 307: 1-14.
- [23] Si XH and Yang LJ. Extraction and purification of TGFbeta and its effect on the induction of apoptosis of hepatocytes. *World J Gastroenterol* 2001; 7: 527-531.
- [24] Dooley S, Delvoux B, Streckert M, Bonzel L, Stopa M, ten Dijke P and Gressner AM. Transforming growth factor beta signal transduction in hepatic stellate cells via Smad2/3 phosphorylation, a pathway that is abrogated during in vitro progression to myofibroblasts. TGFbeta signal transduction during transdifferentiation of hepatic stellate cells. *FEBS Lett* 2001; 502: 4-10.
- [25] Hernandez-Gea V and Friedman SL. Pathogenesis of liver fibrosis. *Annu Rev Pathol* 2011; 6: 425-456.
- [26] Gressner AM and Weiskirchen R. Modern pathogenetic concepts of liver fibrosis suggest

- stellate cells and TGF-beta as major players and therapeutic targets. *J Cell Mol Med* 2006; 10: 76-99.
- [27] Meyer C, Meindl-Beinker NM and Dooley S. TGF-beta signaling in alcohol induced hepatic injury. *Front Biosci (Landmark Ed)* 2010; 15: 740-749.
- [28] Mu M, Zuo S, Wu RM, Deng KS, Lu S, Zhu JJ, Zou GL, Yang J, Cheng ML and Zhao XK. Ferulic acid attenuates liver fibrosis and hepatic stellate cell activation via inhibition of TGF- $\beta$ /Smad signaling pathway. *Drug Des Devel Ther* 2018; 12: 4107-4115.
- [29] Falk P, Angenete E, Bergström M and Ivarsson ML. TGF- $\beta$ 1 promotes transition of mesothelial cells into fibroblast phenotype in response to peritoneal injury in a cell culture model. *Int J Surg* 2013; 11: 977-982.

**Table S1.** Primer sequences for PCR amplification

mRNA	Primer sequence
TGF- $\beta$ 1	Forward primer: AGGGCTACCATGCCAACTTC Reverse primer: CCACGTAGTAGACGATGGGC
Smad2	Forward primer: GGACACGAACTCAAGCGCAA Reverse primer: AATCGGAAGGGAAACGTCGC
Smad3	Forward primer: AGTAAAAGCGAAGTTCGGGC Reverse primer: CTTGGTGTTCACGTTCTGCG
GAPDH	Forward primer: CCGCATCTTCTTGTGCAGTG Reverse primer: ACCAGCTTCCATTCTCAGC

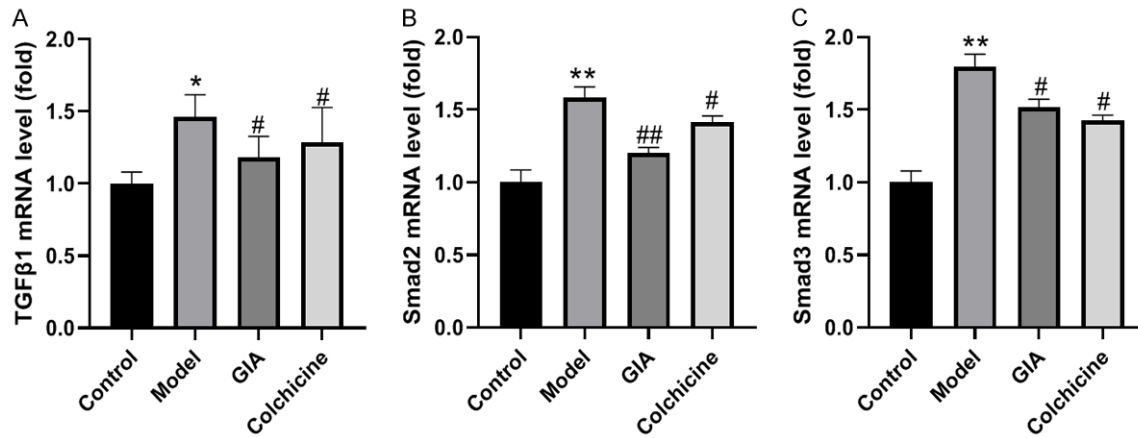


**Figure S1.** The mRNA levels of TGF- $\beta$ 1 (A), Smad2 (B) and Smad3 (C) were quantified by real-time PCR. Compared with the control group \* $P$ <0.05, \*\* $P$ <0.01, compared with the model group # $P$ <0.05, ## $P$ <0.01,  $n$ =3.